1 **Protein Coronas on Functionalized Nanoparticles Enable Quantitative**

2 **and Precise Large-Scale Deep Plasma Proteomics**

3

4 Ting Huang[#,1], Jian Wang[#,1], Alexey Stukalov[1], Margaret K. R. Donovan[1], Shadi Ferdosi[1], Lucy

5 Williamson[1], Seth Just[1], Gabriel Castro[1], Lee S. Cantrell[1], Eltaher Elgierari[1], Ryan W. Benz[1],

6 Yingxiang Huang[1], Khatereh Motamedchaboki[1], Amirmansoor Hakimi[2], Tabiwang Arrey[3], Eugen

7 Damoc[3], Simion Kreimer[4], Omid C. Farokhzad[1], Serafim Batzoglou[1], Asim Siddiqui[1,*], Jennifer

8 E. Van Eyk[4], Daniel Hornburg[1,*]

9

10 [1]Seer, Inc., Redwood City, CA, 94065 USA; [2]Thermo Fisher Scientific, San Jose, CA, USA,

11 [3]Thermo Fisher Scientific, (Bremen) GmbH, Germany; [4]Advanced Clinical Biosystems Research

12 Institute, Precision Health, Barbra Streisand Women's Heart Center at the Smidt Heart Institute,

13 Cedars-Sinai Medical Center, 127 S. San Vicente Blvd., Los Angeles, CA, 90048, USA

14

15 **Correspondence**: Asim Siddiqui (asiddiqui@seer.bio) or Daniel Hornburg

16 (dhornburg@seer.bio), Seer, Inc., Redwood City, CA, 94065 USA

17 **# Equal Contribution**

18 **Keywords**: Proteomics, quantification, plasma, LC-MS, cohort, nanoparticles, clinical proteomics

19 **Word count**: 3543

20 **Figures**: 6

21   **Abbreviations:** nanoparticle (NP), mass spectrometry (MS), liquid chromatography mass

22   spectrometry (LC-MS), data-independent acquisition (DIA), etheylenediaminetetraacetic acid

23   (K_2EDTA), Citrate Phosphate Dextrose (CPD), formic acid (FA), acetonitrile (ACN), Limits of

24   detection (LoD), coefficient of variation (CV), interquartile range (IQR), multiple reaction

25   monitoring (MRM), quality control (QC)

26

Abstract

Background: The wide dynamic range of circulating proteins coupled with the diversity of proteoforms present in plasma has historically impeded comprehensive and quantitative characterization of the plasma proteome at scale. Automated nanoparticle (NP) protein corona-based proteomics workflows can efficiently compress the dynamic range of protein abundances into a mass spectrometry (MS)-accessible detection range. This enhances the depth and scalability of quantitative MS-based methods, which can elucidate the molecular mechanisms of biological processes, discover new protein biomarkers, and improve comprehensiveness of MS-based diagnostics.

Methods: Investigating multi-species spike-in experiments and a cohort, we investigated fold-change accuracy, linearity, precision, and statistical power for the using the Proteograph™ Product Suite, a deep plasma proteomics workflow, in conjunction with multiple MS instruments.

Results: We show that NP-based workflows enable accurate identification (false discovery rate of 1%) of more than 6,000 proteins from plasma (Orbitrap Astral) and, compared to a gold standard neat plasma workflow that is limited to the detection of hundreds of plasma proteins, facilitate quantification of more proteins with accurate fold-changes, high linearity, and precision. Furthermore, we demonstrate high statistical power for the discovery of biomarkers in small- and large-scale cohorts.

Conclusions: The automated NP workflow enables high-throughput, deep, and quantitative plasma proteomics investigation with sufficient power to discover new biomarker signatures with a peptide level resolution.

Introduction

Proteomes are challenging to study due to their complex biochemistry and extensive dynamic range in which protein concentrations vary greatly. For instance, in plasma, 22 blood proteins constitute about 99% of the protein mass, and the remaining 1% consists of thousands of distinct lower abundant proteins and their proteoforms (1). We recently introduced a nanoparticle (NP) protein corona-based workflow that alleviates the dynamic range challenges by compressing it to a more accessible scale at the nano-bio interface (2–4). This novel combination of protein coronas and the unbiased liquid chromatography mass spectrometry (LC-MS) readout has been demonstrated to provide an unprecedented depth at scale leading to new biological insights (2,3,5).

Protein quantification in complex samples, which is essential for capturing biology, can be challenging and has been explored in multiple studies using LC-MS workflows (6–9). Quantification performance can be evaluated at the level of precision and accuracy (**Figure 1A**). Furthermore, accuracy can be dissected into three distinct facets: absolute accuracy, which pertains to protein concentration; relative fold-change accuracy, which provides an accurate estimation of protein up- or down-regulation within a given sample; and linearity, which ensures consistent patterns of up- and down-regulation across various samples for each protein (**Figure 1B**). To discover biological signals, it is primarily important that measured fold-changes follow systematic trends. For instance, the signal should be linear on a logarithmic scale and if desired, calibration functions can be employed to enhance fold-change accuracy or to determine analyte concentrations, thereby refining the overall quantification process (**Figure 1Biv**).

While NP-coronas can overcome the fundamental bottleneck of the plasma's wide dynamic range by compressing it at the nano-bio interface, it is important to understand the quantification

71 performance of this workflow. This motivated us to evaluate the proteome-wide quantification

72 performance of the NP corona-based plasma workflow in terms of relative fold-change accuracy,

73 linearity, and precision. We employed the Proteograph™ Product Suite with the data-independent

74 acquisition (DIA) method to analyze a modified version of the gold standard multi-species

75 proteome spike-in experiment (Experimental overview shown in **Figure 2A, B**) (8,10).

76 Additionally, we investigated assay variance across a 200-sample cohort (over 1,000 LC-MS runs)

77 to evaluate precision of the NP corona-based proteomics workflow and statistical power to detect

78 even small fold-changes reliably.

79

Study design

We evaluated the quantification performance of a NP-corona based workflow by assessing relative fold-change accuracy and linearity using a modified version of the gold standard multi-proteome spike-in experiment (10,11) (**Figure 2A**). Specifically, to evaluate both large and small fold-changes, bovine plasma samples were mixed with two pooled human plasma sample (referred to as IP10 and PC6) at seven different Bovine:Human ratios (1:0, 1:1, 1:1.5, 1:2, 1:9, 1:99, 0:1). We assessed the seven Bovine:Human mixed samples using the fully automated Proteograph workflow (**Figure 2B**), as well as a reference neat plasma workflow. The neat plasma workflow provides a baseline plasma LC-MS proteomics performance since it involves minimal processing steps, no protein coronas, but is limited to high abundance proteins. Additionally, we evaluated the precision of quantification across a cohort of 200 subjects (more than 1000 MS injections) to determine the statistical power of Proteograph in cohorts.

Materials and Methods

93

Spike-in Experiment

94

95 K_2EDTA bovine plasma (Innovative Research, USA) was spiked into two different pooled human

96 plasma samples (IP10 collected in K_2EDTA, and PC6 collected in anticoagulant citrate phosphate

97 dextrose (cpd) tubes) with the following vol/vol ratios of (Bovine:Human) 1:0, 1:1, 1:1.5, 1:2, 1:9,

98 1:99, 0:1 in multi-day quadruplicates. Each replicate of each dilution and sample set was processed

99 as a separate automated Proteograph™ run (V1.2, S55R1100), along with its neat plasma digest.

100 Equal volumes of the peptide elution were dried down in a SpeedVac (3 hours-overnight), and

101 peptides were stored at -80 °C before reconstitution in 20 ul 0.1% formic acid (FA) and 3%

102 acetonitrile (ACN) and LC-MS analysis.

High-Throughput Capillary Flow DIA LC-MS Analysis

103

104 For analysis on the Orbitrap Exploris 480 mass spectrometer (Thermo Fisher Scientific), peptides

105 were loaded on an Acclaim™ PepMap™ 100 C18 (0.3 mm ID x 5 mm) trap column and then

106 separated on a 50 cm µPAC™ HPLC column (Thermo Fisher Scientific) at a flow rate of 1

107 µL/minute using a gradient of 5-25% solvent B (0.1% FA, 100 % ACN) in solvent A (0.1% FA,

108 100% water) over 22 minutes, resulting in a 33-minute total run time. 150-400 ng of material per

109 NP were analyzed in DIA mode using 10 m/z isolation windows from 380-1000 m/z. MS^1 scans

110 were acquired at 60k resolution and MS^2 at 30k resolution.

111 The DIA LC-MS data were analyzed using DIA-NN v1.8 (12) in library-free mode and searched

112 against Uniprot Human plus Bovine protein database (105,533 entries). The following parameters

113 were used: "--mass-acc-ms1 10 --mass-acc 10 --qvalue 0.01 --matrices --missed-cleavages 2 --

114 met-excision --cut K*, R* --smart-profiling --relaxed-prot-inf --pg-level 1 --reannotate"; the

115   remaining parameters were set to default. The false discovery rate (FDR) cutoffs at precursor and

116   protein levels were set to 1%. Most analyses were based on species specific (unique) peptides and

117   proteins. Details of downstream statistical analyses are shared in the supplementary information

118   'LC-MS Data Analysis Exploris 480 MS (supplementary information)'.

119   **Nanoparticle Workflow LC-MS comparison**

120   For the Orbitrap Astral mass spectrometer (Thermo Fisher Scientific), peptides were loaded onto

121   a µPAC™ Neo trap column (Thermo Fisher Scientific) at a flow rate of 1 µL/minute using a

122   gradient of 5-22.5% solvent B (0.1% FA, 100 % ACN) in solvent A (0.1% FA, 100% water) over

123   13 minutes, resulting in a 20-minute total run time. 400 ng of material per injection was analyzed

124   in DIA using 3 m/z isolation windows from 380-980 m/z. MS1 scans were acquired at 240k

125   resolution and MS2 at >80k resolution. For comparison search, LC-MS/MS data were analyzed

126   using DIA-NN v1.8.1 (12) in library free mode and searched against the same Uniprot Human

127   database (48,957 entries) as used for the Orbitrap Exploris 480 analysis (no matching between

128   runs). The following parameters were used: "--matrices --met-excision --cut K*, R* --relaxed-

129   prot-inf --pg-level 1 --individual-mass-acc --individual-windows "; the remaining parameters were

130   set to default. FDR cutoffs at precursor and protein levels were set to 1%.

131   **Reproducibility Study**

132   A control pooled human plasma sample was processed with two different Proteograph SP100

133   automation instruments, on two separate days each, resulting in a total of 4 batches (plates). Tryptic

134   peptides from 6 replicates were analyzed using the same set up as outlined above with an Orbitrap

135   Exploris 480 Mass Spectrometer here in DDA mode with a 30-minute LC gradient. LC-MS data

136   files were processed using Proteograph Analysis Suite (PAS MaxQuant module), with 1% FDR at

137   the protein and peptide levels (13). Coefficient of variance (CV) were evaluated on median

138   normalized peptide intensities for peptides found in 3 or more replicates, with four different

139   replicate grouping methods: within plate (batch), within day across SP100 instruments, within

140   SP100 across days, and between days and SP100 instruments.

141   **Cohort Study**

142   A pooled human plasma (process quality control (QC)) sample, consisting of pre-pooled K_2EDTA

143   plasma from ProMedDx (Norton, MA) derived from healthy subjects, was processed as control on

144   each Proteograph Assay plate analyzed across 200 plasma cohort samples (1- 3 controls included

145   on 14 plates on three Proteograph SP100 automation instruments) resulting in 117 QC

146   measurements. Peptides were loaded on an Acclaim PepMap 100 C18 (0.3 mm ID x 5 mm) trap

147   column and then separated on a 50 cm µPAC analytical column (Thermo Fisher Scientific) at a

148   flow rate of 1 µL/minute using a gradient of 5 – 25% solvent B (0.1% FA, 100 % ACN) in solvent

149   A (0.1% FA, 100% water) over 42 minutes (63-minutes total run time) on two different timsTOF

150   Pro mass spectrometers (Bruker). A total of 200 ng of peptides per NP was analyzed in ddaPASEF

151   mode using ion mobility range of 0.85 – 1.30 V.s/cm² with 100 ms accumulation time. DDA data

152   were analyzed with MSFragger 3.4 using the default settings in PAS, based on the Uniprot Human

153   FASTA database (see above). Peptide intensity CVs were calculated based on median normalized

154   intensities for peptides found in 3 or more replicates to represent the variability of performance

155   across and within the two LC-MS systems during this cohort study. Statistical details are shared

156   in the supplementary information 'Cohort Study (supplementary information)'.

157 **Reference Spike-in Experiment**

158 We compared the Proteograph workflow performance to published work (37), where Tognetti et

159 al. had evaluated the performance of a plasma depletion workflow using a controlled spike-in

160 experiment. Human plasma background was spiked with fixed ratios into Saccharomyces

161 cerevisiae (1:1.3) and Escherichia coli (1:0.5), each in 20 technical replicates. For our comparison,

162 we obtained the Spectronaut precursor reports for both the depletion and neat workflows from the

163 MassIVE repository (dataset ID: MSV00088180). The precursor-level fold-changes between two

164 conditions were calculated and compared to the spiked-in ratios of corresponding proteomes. To

165 make the fold-change errors more comparable to the 4 replicates used in our study, we

166 downsampled the data to four replicates randomly 100 times and took the mean fold-change error

167 for each precursor.

168 Results

169 High proteome coverage and precision of NP-based workflows

170 Compared to the neat plasma workflow, the compression of dynamic range in NP-protein coronas

171 results in significantly higher coverage of proteomes (2,3,14). Importantly, absolute proteome

172 depths and fold improvements depend on plasma sample complexity and specifics of the LC-MS

173 workflow. For instance, Proteograph in conjunction with the latest Thermo Scientific Orbitrap

174 Astral Mass spectrometer reveals more than 6,000 proteins and 50,000 precursors in plasma

175 compared to only hundreds of proteins accessible with a traditional upfront neat plasma workflow

176 (**Figure 3A**). To evaluate the quantitative performance of a NP workflow, we evaluated a set of

177 mixed species proteome experiments on the Orbitrap Exploris 480 system to a depth of more than

178 3000 proteins across all dilutions (**Figure 3B**). Importantly, a stringent 1% false discovery rate for

179 the identification at precursor and protein level was applied in every analysis. Moreover, while the

180 mixed species experiments are well established to investigate quantification, these analyses require

181 additional filtering steps including the removal of shared proteins and peptides, or detection across

182 the entire range of the dilutions, which reduces the reported unique protein identifications. The NP

183 workflow provides more measurements at any quantification stringency and every spike-in ratio

184 (**Figure 3C, D**). For example, at 1:1 spike-in ratio, a median of 268% more proteins were

185 quantified using the NP workflow compared to neat plasma digestion (395 vs. 1,058) with the CV

186 of protein intensities across four assay replicates below 20% (**Figure 3D**). Proteins detected in

187 both, NP-based and neat plasma digestion workflows, show similar or slightly increased CVs on

188 Proteograph (**Figure 3D**). Overall, these results demonstrate superior NP performance yielding

189 more proteins than neat plasma alone with high precision and for shared proteins, showing

190 comparable reproducibility.

191

Fold-change Accuracy of Workflows

193 For accuracy and linearity evaluation we restricted our analysis to bovine-specific peptides and

194 proteins as wider range of bovine concentrations measured allowed more robust estimations. To

195 evaluate the relative fold-change accuracy of the NP workflow, we compared the measured fold-

196 changes (observed change in protein intensities between spike-in ratios) with expected fold-

197 changes (expected change in protein concentrations between spike-in ratios) of bovine proteins in

198 15 pairwise comparisons with 6 different spiked-in ratios. **Figure 4A, B** shows the results for three

199 pairs of bovine spike-in ratios (2:1, 5:1, and 10:1), and the results for all 15 comparisons are shown

200 in **Supplementary Figure 1.** The median fold-change is consistent across dilutions for both, the

201 reference NP and neat digestion workflows, with a wider spread of fold-changes for the NP

202 workflow. The expected fold-change is within the interquartile range (IQR) in most cases. For

203 high dilutions, fold-change accuracy is increased for proteins quantified based on more than 1

204 peptide (**Supplementary Figure 1**) demonstrating the utility of quantifying multiple peptides per

205 protein. Importantly, at any fold-change accuracy threshold NPs quantify more proteins than the

206 reference neat plasma workflow (**Figure 4C, Supplementary Figure 2**). For the biosample PC6,

207 we observed slightly decreased accuracy (**Supplementary Figure 3**). This pooled human blood

208 plasma was collected differently than bovine plasma (CPD *vs.* K_2EDTA) resulting in a variable

209 buffer background across spike-in ratios. This appears to reduce accuracy and, since buffers

210 mixing does not take place in clinical studies, we focus on IP10 (K_2EDTA) for the remaining

211 analyses.

212 A recently published study (15) compared a multi-step depletion workflow with neat

213 plasma. Despite differences in biosamples, LC-MS methods, spike-in ratios, and computational

214   pipelines, the fold-change distributions are comparable for similar spike-in ratios (**Supplementary**

215   **Figure 4)**. Together, these results demonstrate NP-coronas capture quantitative differences across

216   a wide range of concentrations and enable identification of substantially more proteins with

217   similarly high quantification accuracy compared to a traditional neat plasma digestion workflow.

218

Linearity of Quantitative Differences

220   Proteins that exhibit lower fold-change accuracy can still be highly valuable if they follow a

221   systematic, e.g., log linear range trend, of quantification. The accuracy analysis (**Figure 4)** shows

222   that, in comparison to a neat workflow, log fold-changes for a subset of proteins measured by the

223   NP workflow can be compressed or inflated, due to the dynamic range compression that achieves

224   much improved access to proteins in complex biosamples. We calculated the Pearson correlation

225   between observed and expected log fold-changes for all proteins detected in the respective assay

226   to evaluate linearity of the response, i.e., estimate how well protein regulation across biosamples

227   can be captured. Across all spiked-in ratios (15 comparisons), we observed high linearity of the

228   NP-workflow with a median Pearson correlation 0.995 that compares 0.998 in neat (**Figure 5A**).

229   As well, most of the shared proteins, show a similar high linearity with slight advantages for the

230   high abundance proteins detected in neat (**Figure 5A**).

231   In line with our observation for fold-change accuracy and consistent with an improved limit

232   of quantification, the NP workflow quantifies more proteins at any linearity threshold. For

233   instance, a stringent Pearson correlation of $\geq$ 0.99 was calculated for consistently detected,

234   bovine-unique proteins across all dilutions. The NP workflow identified 113 such proteins,

235   compared to 68 proteins detected by the neat plasma workflow (**Figure 4B**). Proteins

236   demonstrating linearity with a Pearson correlation < 0.9 were minimal, 3 out of 83 for neat plasma,

237   25 out of 182 for NP, and 4 out of 70 for the shared proteins.

238   A key advantage of MS-based proteomics is to detect and quantify proteins through

239   independent measurements of multiple peptides comprising unique amino acid sequences. This

240   opens the opportunity to target peptides that present high linearity for efficient multiple reaction

241   monitoring (MRM) MS acquisition. To compare quantitative performance of the 'best' peptides for

242   human biomarker proteins mapped to bovine protein gene names, we selected the most linear

243   peptide from two assay replicates based on Pearson correlation p-value. Subsequently, we

244   evaluated linearity for these peptides in the remaining replicates (**Figure 5C**). The results

245   demonstrated good linearity for both workflows, excluding Q3SZ57 (AFP), identified as a

246   common outlier.

247   Despite the NP workflow's design intent to significantly lower the signal (i.e., mass) for

248   high-abundant proteins and thus, enhance the detection of low abundant content of proteomes, the

249   signal maintained robust linearity for both proteins and peptides. This finding underscores NP's

250   utility for capturing proteins and quantifying dynamics across low and high abundance proteins

251   (**Figure 4C, 5B,C**). Furthermore, the high degree of linearity indicates that further accuracy

252   enhancements may be attained through additional normalization in both the neat plasma and NP-

253   based workflows. Indeed, employing a simple linear fit correction for individual precursors, we

254   were able to increase the fold-change accuracy in the NP workflow by a median of 34.1% across

255   the dynamic range (**Supplementary Figure 5**).

256

257 **Statistical Power in Large-scale Studies**

258 All steps of a proteomics workflow, including sample preparation, chromatography, and MS, can

259 contribute to variation in results. To dissect individual steps in the workflow, we evaluated how

260 CVs change with each workflow component (**Figure 6A**). For LC-MS reinjection alone, we

261 observed a CV of 8.9% while the CV for the full workflow was 16.8% within batch and 20.9%

262 across batches (including corona formation, protein digestion, peptide cleanup, different SP100

263 instruments and Proteograph Assay Kits on different days). Thus LC-MS accounts for about half

264 of the overall variation (**Figure 6B**).

265 To estimate the precision of NP-workflow across an entire biomarker study, we compared the

266 performance for 117 plasma quality control (QC) samples versus 1,000 injections of 200 unique

267 biosamples. This allowed us to compare QC-samples across 14 Proteograph assay (sample

268 preparation) runs and peptides analyzed on two distinct LC-MS systems (**Figure 6C**). The QC

269 variance accumulated over time to around 24% for a single LC-MS system and 28.5% across two

270 LC-MS systems (**Figure 6D**). Importantly, this is substantially lower than the combination of

271 biological and technical variation observed here and in other proteomics studies which is larger

272 than 40% (41,42). We also estimated the statistical power to detect protein abundance differences

273 based on the average variance across QC samples (28.5%), as well as patient samples (53.1%)

274 with and without controlling for known assay variables such as sample preparation batch and LC-

275 MS system. To detect biological differences of 2× at a stringent false discovery rate of 5% less

276 than 30 samples (per group) are required in this cohort. If the biological background heterogeneity

277 is low (e.g., for cell lines) the statistical power can depend more on technical variance. We

278 approximated such cases considering the variance across all QC samples and determined that for

279 detecting a 2× difference only 4 (controlling for assay variables) samples would be required, and

280   10 samples provide sufficient statistical power to detect fold-changes as little as 1.5× with high

281   statistical confidence (**Figure 6E**). Together, this demonstrates sufficient reproducibility of the

282   NP-workflow in large and small-scale studies to detect even small protein abundance differences.

283

Discussion

Deep, unbiased access to the entire dynamic range of the plasma proteome at scale has great potential to advance our understanding of the proteome dynamics in health and disease. Previously, we have shown that NP-coronas compress the wide dynamic range of the plasma proteome, enabling deep and broad access to plasma proteins (3,14) at a scale to detect novel biomarkers (2,5). We have also shown that the high-throughput NP-based workflow provides quantitative response similar to ELISA assay, exemplified by four proteins (CRP, S100a8, S100a9, ANG) spiked in plasma at five different biologically relevant concentrations (2). Here, we conducted a comprehensive, proteome-wide evaluation of precision of quantification, fold-change accuracy, and linearity of log fold-changes as well as statistical power in cohort studies.

The utilization of multi-species plasma mixtures and the use of MS to evaluate quantification has several advantages over other approaches used to assess quantification and linearity. Firstly, measurements with ELISA may be subject to proteoform effects that are hard to distinguish from measurement error. For that reason, MS is used as a gold standard validation strategy for targeted affinity based capture assays (16,17). While NPs may sense proteoforms, the MS readout is more likely to resolve signal from multiple protein variants. Secondly, the multi-species approach allows us to simultaneously evaluate the quantification across many peptides of many proteins across the entire detection range rather than be limited to a few spiked-in proteins. Together, it allows us to more accurately estimate real world quantification accuracy in complex, plasma samples than would be achieved through individual measurements of isolated analytes.

The advantage of NPs compressing the dynamic range—i.e., transforming the absolute protein quantification (concentration)—is that it allows for unprecedentedly deep access to the

306   dynamic range at scale without the need to target specific proteins of interest (unbiased approach).

307   By design, NPs reduce the signal of high abundance proteins, such as albumin (signal

308   compression), to capture more low abundance ones, like chemokines (signal enhancement). Our

309   data demonstrate that, protein coronas not only render proteome content more visible to

310   downstream detectors but also capture quantitative differences across samples with greater

311   numbers of proteins and peptides at high precision, fold-change accuracy, and linearity. Moreover,

312   the high linearity of the log fold-change response across a wide range of spiked-in ratios offers a

313   clear path to combine NPs with rapid a MRM-based acquisition targeting highly quantitative

314   peptides and further enhance fold-change accuracy by calibrating measured proteins and peptide

315   intensities.

316   The feasibility of comprehensive biomarker discovery studies, spanning hundreds to

317   thousands of plasma samples from human subjects or animal models, paves the way for the

318   identification of a multitude of novel biomarkers. As we and other demonstrated previously, this

319   is especially true within the traditionally challenging low-abundance range of the plasma proteome

320   (4,18,19). Across such studies, high precision of quantification must be maintained, which we

321   demonstrate in a 200-subject, 1000-sample pilot study is now possible using the automated NP

322   workflow. Importantly, our analysis demonstrates that the technical variance even in large-scale

323   studies comparing data across multiple instruments is substantially lower than the biological signal

324   resulting in sufficient statistical power to discern even small biologically relevant protein

325   abundance differences. Notably, not all biological variance is related to the phenotype under

326   investigation and potential confounding factors may not always be identifiable or controllable

327   (e.g., using models that control for age or BMI). This increases the necessity for larger-scale

328   studies for complex human biology, underscoring the importance of workflows capable of

329   accommodating thousands of samples. Collectively, our findings underscore the quantitative

330   performance of protein corona-based assays, which holds significant opportunities for large scale,

331   quantitative proteomics studies and biomarker discovery.

332

Authors Disclosure or Potential Conflict of Interest

O.C.F. has financial interest in Selecta Biosciences, Tarveda Therapeutics, and Seer where he is officer/director; and he serves as Senior Lecturer at BWH/HMS. S.F., Al.St., M.H., B.T., T.R.B., T.W., E.M.E., X.Z., E.S.O., A.A., B.L., J.C., M.F., J.W., M.G., H.X., C.S., Y.H., S.B., A.S., V.F., O.C.F., D.H. have financial interest in Seer, S.F., B.T., T.R.B., T.W., E.M.E., E.S.O., X.Z., T.W., J.C., M.F., J.W., M.G., H.X., C.S., A.S., V.F., O.C.F., D.H. have financial interest in PrognomiQ. E.D., T.A., A.H. are employed by Thermo Fisher Scientific. R.W. is a consultant to ModeRNA, Lumicell, Seer, Earli, and Accure Health. All other authors declare no conflicts of interest.

Acknowledgment

Author Declaration

All authors confirmed they have contributed to the intellectual content of this paper with significant contributions to the conception and design, acquisition of data, or analysis and interpretation of data; drafting or revising the article for intellectual content; final approval of the published article; and agreement to be accountable for all aspects of the article thus ensuring that questions related to the accuracy or integrity of any part of the article are appropriately investigated and resolved.

References

1. Bollineni RC, Guldvik IJ, Grönberg H, Wiklund F, Mills IG, Thiede B. A differential protein solubility approach for the depletion of highly abundant proteins in plasma using ammonium sulfate. Analyst. 2015;140:8109–17.

2. Blume JE, Manning WC, Troiano G, Hornburg D, Figa M, Hesterberg L, et al. Rapid, deep and precise profiling of the plasma proteome with multi-nanoparticle protein corona. Nat Commun. 2020;11:3662.

3. Ferdosi S, Tangeysh B, Brown TR, Everley PA, Figa M, McLean M, et al. Engineered nanoparticles enable deep proteomics studies at scale by leveraging tunable nano–bio interactions. Proc Natl Acad Sci United States Am. 2022;119:e2106053119.

4. Ferdosi S, Stukalov A, Hasan M, Tangeysh B, Brown TR, Wang T, et al. Enhanced Competition at the Nano–Bio Interface Enables Comprehensive Characterization of Protein Corona Dynamics and Deep Coverage of Proteomes (Adv. Mater. 44/2022). Adv Mater. 2022;34:2270307.

5. Donovan MKR, Huang Y, Blume JE, Wang J, Hornburg D, Mohtashemi I, et al. Peptide-centric analyses of human plasma enable increased resolution of biological insights into non-small cell lung cancer relative to protein-centric analysis. Biorxiv. 2022;2022.01.07.475393.

6. Aebersold R, Mann M. Mass spectrometry-based proteomics. Nature. 2003;422:198–207.

7. Ong S-E, Mann M. Mass spectrometry–based proteomics turns quantitative. Nat Chem Biol. 2005;1:252–62.

8. Pino LK, Rose J, O'Broin A, Shah S, Schilling B. Emerging mass spectrometry-based proteomics methodologies for novel biomedical applications. Biochem Soc T. 2020;48:1953–66.

9. Cox J, Hein MY, Luber CA, Paron I, Nagaraj N, Mann M. Accurate Proteome-wide Label-free Quantification by Delayed Normalization and Maximal Peptide Ratio Extraction, Termed MaxLFQ*. Mol Cell Proteomics. 2014;13:2513–26.

10. Navarro P, Kuharev J, Gillet LC, Bernhardt OM, MacLean B, Röst HL, et al. A multicenter study benchmarks software tools for label-free proteome quantification. Nat Biotechnol. 2016;34:1130–6.

11. Pino LK, Searle BC, Yang H-Y, Hoofnagle AN, Noble WS, MacCoss MJ. Matrix-Matched Calibration Curves for Assessing Analytical Figures of Merit in Quantitative Proteomics. J Proteome Res. 2020;19:1147–53.

385 12. Demichev V, Messner CB, Vernardis SI, Lilley KS, Ralser M. DIA-NN: neural networks and
386   interference correction enable deep proteome coverage in high throughput. Nat Methods.
387   2020;17:41–4.

388 13. Cox J, Mann M. MaxQuant enables high peptide identification rates, individualized p.p.b.-
389   range mass accuracies and proteome-wide protein quantification. Nat Biotechnol. 2008;26:1367–
390   72.

391 14. Ferdosi S, Stukalov A, Hasan M, Tangeysh B, Brown TR, Wang T, et al. Enhanced
392   Competition at the Nano–Bio Interface Enables Comprehensive Characterization of Protein
393   Corona Dynamics and Deep Coverage of Proteomes. Adv Mater. 2022;34:e2206008.

394 15. Tognetti M, Sklodowski K, Müller S, Kamber D, Muntel J, Bruderer R, et al. Biomarker
395   Candidates for Tumors Identified from Deep-Profiled Plasma Stem Predominantly from the Low
396   Abundant Area. J Proteome Res. 2022;21:1718–35.

397 16. Raffield LM, Dang H, Pratte KA, Jacobson S, Gillenwater LA, Ampleford E, et al.
398   Comparison of Proteomic Assessment Methods in Multiple Cohort Studies. Proteomics.
399   2020;20:e1900278.

400 17. Candia J, Daya GN, Tanaka T, Ferrucci L, Walker KA. Assessment of variability in the
401   plasma 7k SomaScan proteomics assay. Sci Rep-uk. 2022;12:17147.

402 18. Anderson NL. The Clinical Plasma Proteome: A Survey of Clinical Assays for Proteins in
403   Plasma and Serum. Clin Chem. 2010;56:177–85.

404 19. Geyer PE, Holdt LM, Teupser D, Mann M. Revisiting biomarker discovery by plasma
405   proteomics. Mol Syst Biol. 2017;13:942.

406

407

408   **Figure Legends**

409   **Figure 1**. **Overview of Quantification Levels and Data Transformation.** (A) Two quantitative

410   performance metrics are: 1) accuracy, measuring how close a measurement is to the true value;

411   and 2) precision, measuring how close are the measurements across replicate analyses. (B) The

412   measurement of two proteins (A, orange, and B, blue) across 3 biosamples (samples #1, #2, and

413   #3) illustrates three layers of quantification accuracy: absolute accuracy (i and ii for untransformed

414   and log-transformed data, respectively), relative fold-change (FC) accuracy (iii), and linearity (iv).

415

416   **Figure 2**. **Study Overview.** (A) Experimental design of the spike-in experiment, in which a bovine

417   plasma proteome is spiked into a human plasma proteome at seven different ratios. (B)

418   Proteograph™ workflow overview which includes protein corona formation, proteins

419   denaturation, reduction, alkylation, protein digestion, and peptide desalting on the Proteograph

420   SP100 automation instrument. Peptides are quantified, dried, and resuspended before injection

421   onto an LC-MS system.

422

423   **Figure 3. Identification and Precision Performance of a Neat Plasma and NP-corona**

424   **Workflow.** (A) Protein (left y-axis) and precursor identifications (right y-axis) determined for

425   different LC-MS setups and biosamples comparing traditional neat workflows and NP workflow.

426   Thermo Scientific Orbitrap Astral MS data was acquired for assay replicates standard deviations

427   indicated by error bars, lower dash denoting identifications shared by all replicates (N=3), upper

428   dash indicates identification across all replicates and nanoparticles. (B) The number of proteins

429   quantified in mixed species plasma experiment on Exploris 480 at each ratio for the NP (teal) and

430   neat workflow (grey), including bovine proteins and human proteins and those that are shared

431   between species. Subsequent plots focused on species specific (unique) peptides and proteins. (C)

432   Lower limits of quantification (LoQ) for bovine proteins quantified in both workflows. LoQ is the

433   lowest level of dilution with a stringent quantitative response (lower is better). (D Number of

434   proteins identified at a given coefficient of variation (CV) threshold for each spiked-in ratio. X-

435   axis is the CV, and the Y-axis is the total number of bovine and human proteins quantified in four

436   replicates with a CV lower than the given threshold. NP-workflow proteins also identified in neat

437   (light teal), NP-workflow with all proteins (dark teal), and neat workflow (grey). Data shown is

438   for IP10 human plasma pool.

439

440   **Figure 4. Fold-change Accuracy Performance of a Neat Plasma and NP-corona Workflow.**

441   (A) Three representative pairs of spiked-in samples and the expected fold-changes of bovine

442   proteins concentration in these pairs. (B) Distribution of observed fold-changes of bovine proteins

443   for 3 selected comparisons of spiked-in samples. The color indicates the data source: neat digestion

444   (grey), Proteograph workflow (dark teal), or Proteograph workflow, but constrained to proteins

445   also identified in neat (light teal). The horizontal dashed lines indicate the expected fold-changes.

446   Boxplots report the 25% (lower hinge), 50%, and 75% quantiles (upper hinge). Whiskers indicate

447   observations equal to or outside hinge $\pm$ 1.5 * interquartile range (IQR). Outliers (beyond 1.5 *

448   IQR) are not plotted. (C) The number of bovine proteins identified at a given accuracy threshold

449   for each expected fold-change. X-axis is the % accuracy error, i.e.,

450    $\left|\log_2 FC_{observed} - \log_2 FC_{expected}\right|/\log_2 FC_{expected}$. The Y-axis is the number of proteins with

451   an accuracy error below the given threshold. The horizontal dashed lines indicate proteins reported

452   at the 25% threshold. Ribbon denotes the 99th confidence interval. Data shown here are based on

453   IP10.

454

455   **Figure 5**. **Linearity of Protein Quantification for Neat and Proteograph Workflows.** Pearson

456   correlation is calculated between observed and expected fold-changes of bovine proteins. (A) Neat

457   digestion correlation versus Proteograph workflow correlation. Each dot represents one bovine

458   protein. The marginal density plots show the distribution of Pearson correlation. 84 bovine proteins

459   detected in all seven spiked-in ratios by both neat digestion (Grey color) and Proteograph

460   workflows (Teal color) were plotted. (B) The number of bovine proteins identified at a given

461   correlation threshold. X-axis is the Pearson correlation (truncated at 0.95), and the Y-axis is the

462   number of bovine proteins with a correlation higher than the given threshold. The horizontal

463   dashed lines indicate the number of proteins with a correlation ≥ 0.99. Proteograph workflow with

464   proteins identified in neat workflow is colored in light teal, Proteograph workflow with all proteins

465   is colored in dark teal, and neat digestion workflow is colored in grey. Data shown here are based

466   on IP10. Plots depict bovine proteins only (identified with at least one bovine-specific peptide)

467   that are detected at least once across all 15 pairwise comparisons. (C) Linearity of biomarkers

468   matched to bovine proteins based on their gene symbols. 32 biomarkers were detected by the NP

469   workflow while 30 biomarkers were detected in neat. Dashed lines connect the estimated fold-

470   changes for each biomarker. Pink dashed line shows common outlier Q3SZ57. Selection of the

471   most linearly responding peptides is based on Pearson correlation p-value determined for two assay

472   replicates for matched biomarkers in neat workflow and NP-workflow. Depicted is the average of

473   the two remaining replicates for the selected peptides.

474

475   **Figure 6**. **Reproducibility and Statistical Power for Proteograph Workflow in large-scale**

476   **Discovery Proteomics Studies.** (A) Experimental design of the reproducibility study. (B) Peptide

477   level CV within and across plates, Proteograph SP100 automation instruments, and days of LC-

478   MS analysis. (C) Experimental design of cohort study. (D) Peptide CV within and across LC-

479   MS/MS instruments. (E) Statistical power analysis for a 200-sample, 1,000 injections cohort study

480   detecting fold-change difference with 5% FDR and a power of 0.8.

481

482 **Figures**

483
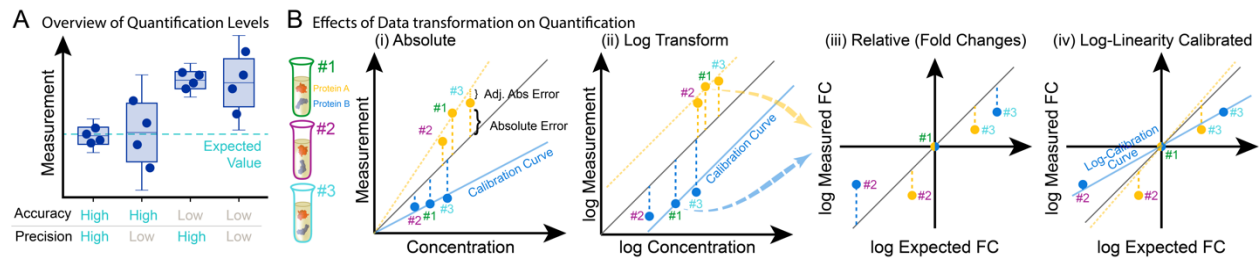
484 Figure 1

485

486
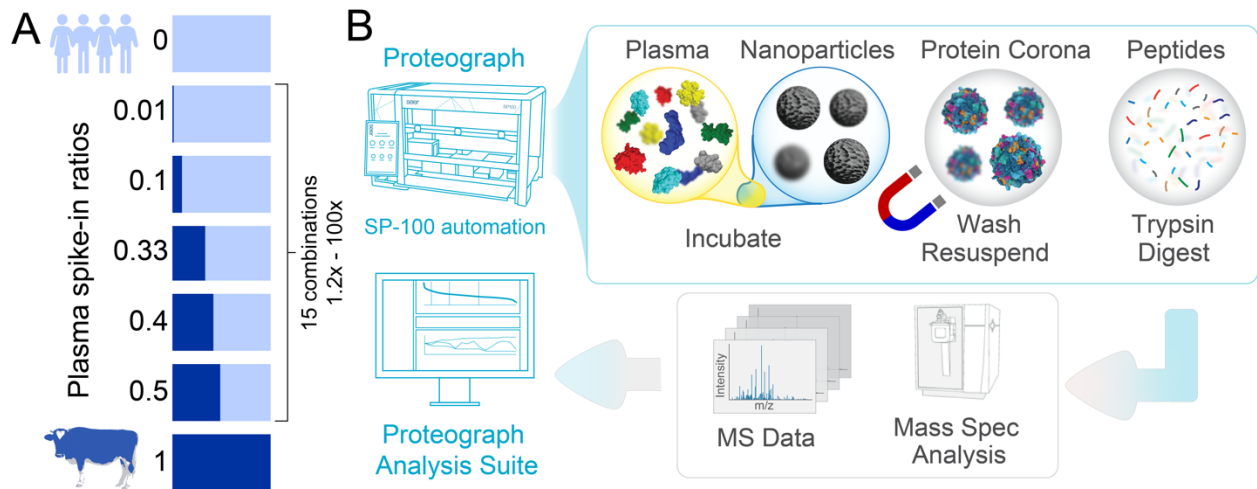
487 Figure 2
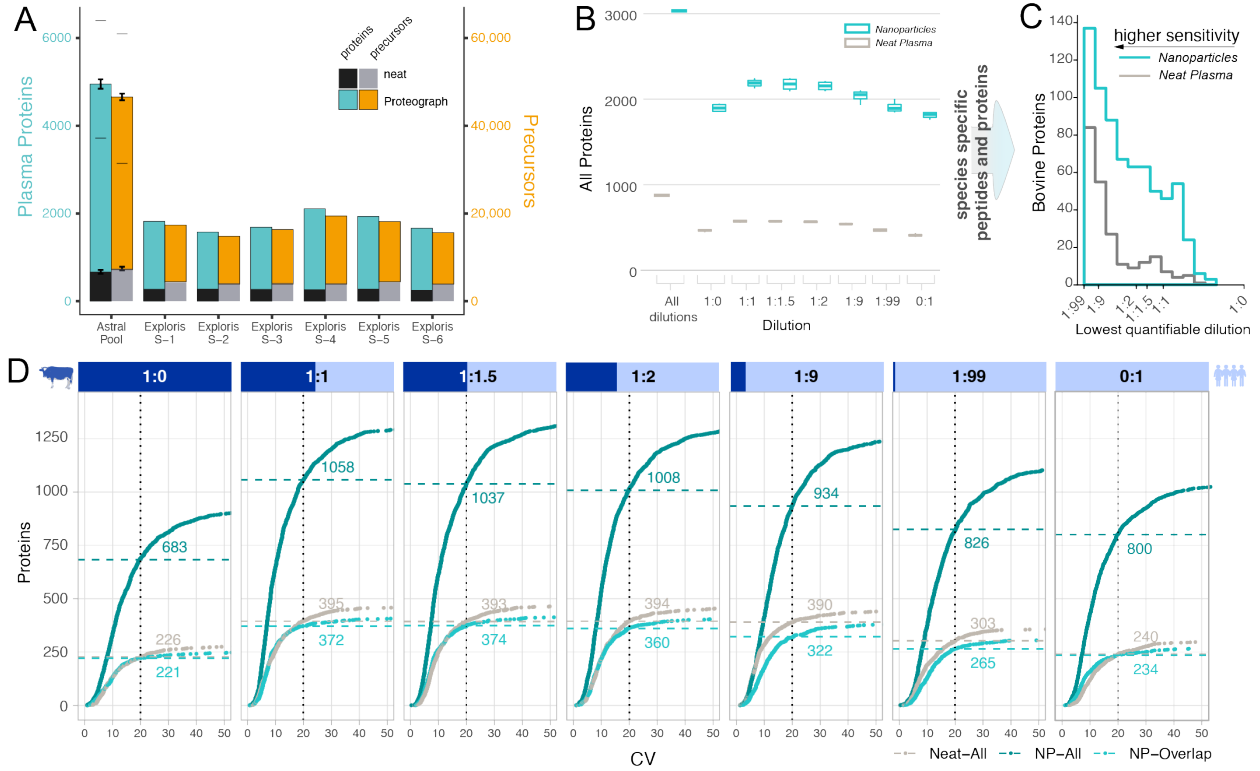
488

489   Figure 3

490

491
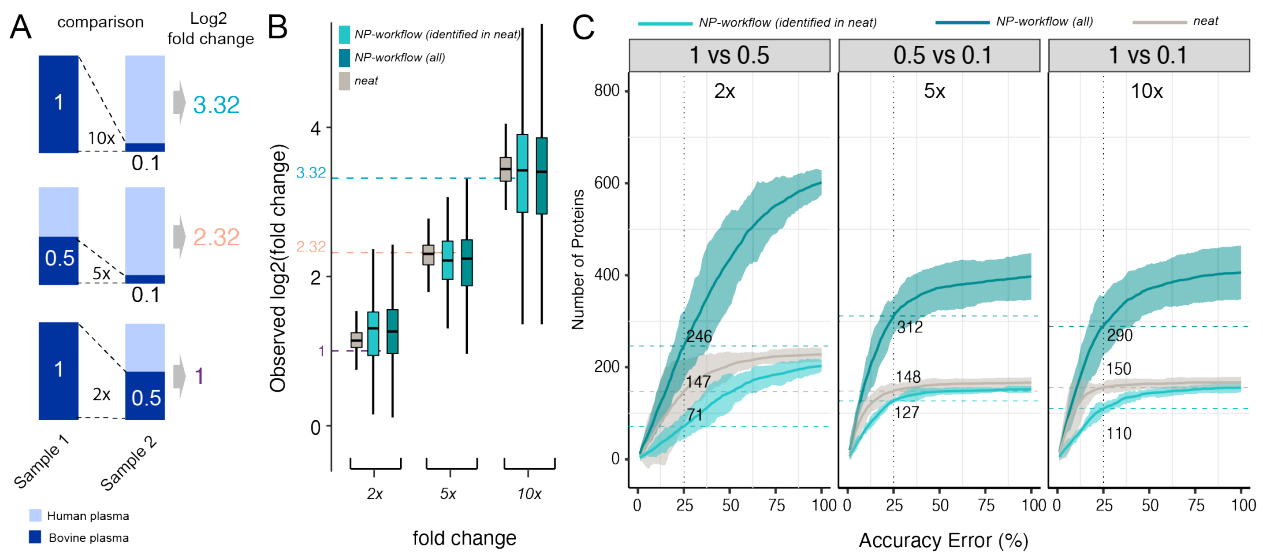
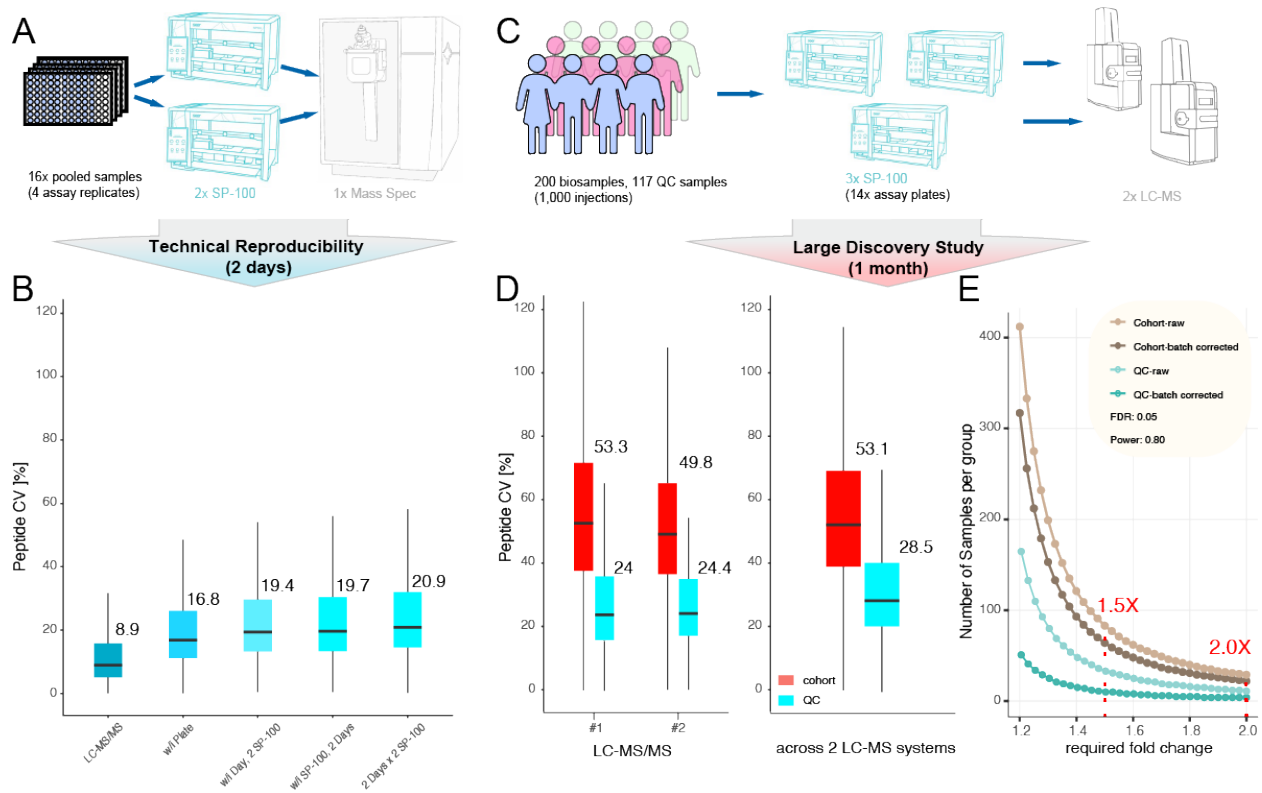492   Figure 4
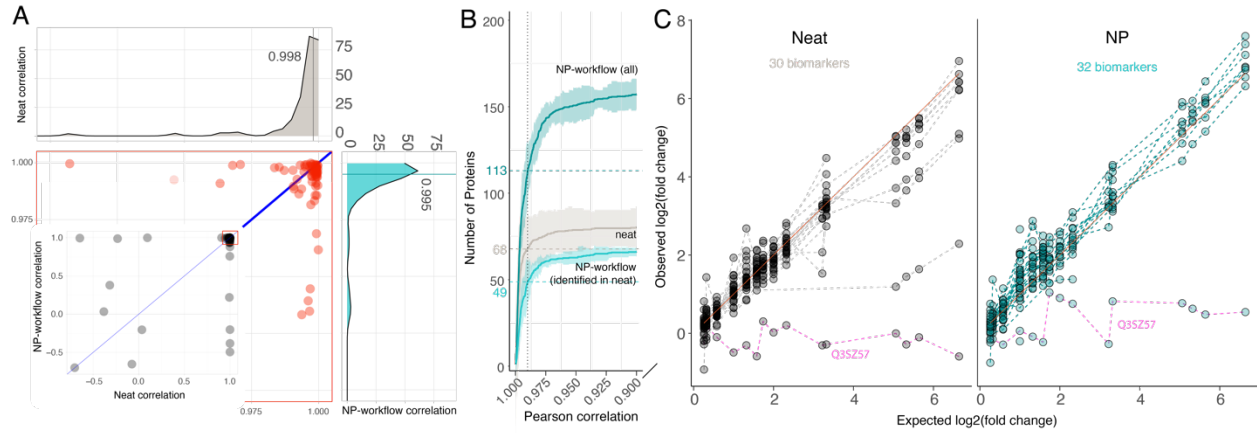
493

494   Figure 5

495

496

497   Figure 6